Subthreshold oscillations of map-based neuron model

ANDREY L. SHILNIKOV
Department of Mathematics and Statistics,
Georgia State University, Atlanta, GA 30303-3083, USA

NIKOLAI F. RULKOV
Institute for Nonlinear Science, UCSD
San Diego, CA 92093-0402, USA

December 3, 2003

Abstract

A map-based model of neuronal behavior with subthreshold oscillations is considered. We discuss bifurcation scenarios of the birth of small subthreshold oscillations and dynamical mechanisms behind transformation of these oscillations into large spikes.

1 Introduction

Studies of dynamical behavior of biological networks require computation of the network models containing a very large number of neurons. Despite the variety of very complex dynamical mechanisms involved in the formation of neuron activity, these studies need simple phenomenological models that captures the basic features of individual neurons provided are simple enough to allow one to perform quick and comprehensive computations of large neural networks. Various ideas for the design of a simple low-dimensional

map for modeling of neuron behavior have been proposed, see for example [1, 2, 3, 4, 5]. Most of these studies focused on the description of either fast spiking activity or slow bursting dynamics neglecting individual spikes.

A simple phenomenological map-based model that can replicate spiking-bursting neural activity has been suggested recently in [6]. This model is a low-dimensional map that is designed to mimic rather realistically various types of transitions occurred in biological neuron. These transition include silence $\leftrightarrow$ tonic spiking as well as a triplet: silence $\leftrightarrow$ bursts of spikes $\leftrightarrow$ tonic spiking. The map is also enable to mimic properly various chaotic regimes of spiking-bursting activity [6]. Such types of phenomenological models are of special interest nowadays as they have very a high potential for development of computationally efficient studies and modeling of functional behavior in large-scale neurobiological networks [7].

The bifurcation analysis of the map model carried out in [8] has shown that the transition from silence to spiking or to busting activity is characterized by a subcritical birth of an unstable invariant closed curve that collapses into the stable fixed point, thereby, terminating its stability. This unstable invariant curve in the map is equivalent to an unstable limit cycle a low-order ODEs model with a similar transition. Therefore, the original map model [6] provides only a dangerous (noninvertible) transition from the regime of silence to spikes as a control parameter (e.g. the depolarization current) passes the threshold. This scenario is quite typical for the most types of the biological neurons. However, the studies suggest besides that some neurons may come out of the silence softly. If it is so there must be small amplitude oscillations existing bellow the threshold of the spike excitation [9]. These subthreshold oscillations of almost sinusoidal form facilitate the generation of spike oscillations when the membrane gets depolarized or hyperpolarized [10, 11] Such almost sinusoidal oscillations play an important role in shaping specific forms of rhythmic activity vulnerable to the noise in the network dynamics [12, 13].

In the given paper we tailor the map so that it admits *stable* subthreshold oscillations. This is due to a suitable alteration of the function in the right hand side of the fast subsystem. We will start with the analysis of local bifurcations of a fixed point. The loss of stability of the latter is accompanied with the birth of the stable invariant circle which will begin a family of canards in the map. While following the further evolution of the circle we rant into another very intriguing phenomenon, namely it breaks down into homoclinic tangles. We will also elaborate on heteroclinic crossings between

the stable and unstable invariant manifolds — the images of the slow motion surface in the singularly perturbed system

2 Map-based model with stable subthreshold oscillations

The neuron model of spiking-bursting oscillations proposed in [6] can be written in the form

$$\bar{x} = f_\alpha(x, y+\beta), \tag{1a}$$
$$\bar{y} = y - \mu(x+1-\sigma), \tag{1b}$$

In it the control parameters α, σ and $0 < \mu \ll 1$ define individual dynamics of the system. The input parameters β and σ are employed to couple a number of such neuron models; they describe the injected current. The principal distinction of (1) from the original map analyzed in [6, 8] is concealed in the shape of the piece-wise continuous function $f_\alpha(x, y+\beta)$ when $x \le 0$. Now the function given by

$$f_\alpha(x, y+\beta) = \begin{cases} -\alpha^2/4 - \alpha + y + \beta, & x < -1 - \alpha/2, \\ \alpha x + (x+1)^2 + y + \beta, & -1 - \alpha/2 \le x \le 0 \\ y + 1 + \beta, & 0 < x < y + 1 + \beta \\ -1, & x \ge y + 1 + \beta \end{cases}, \tag{2}$$

looks as follows in Fig. 1.

The function has discontinuity at $x = y + 1 + \beta$ which belongs to the last interval where the function does not change. This shape of the function is used to achieve a generation of sharp spikes in the map. The top of the spike corresponds to the iteration which has the value of x in the most right interval. Slow variable y can turn the spike generator on or off. It also describes some adaptation processes in the neuron dynamics.

The second interval ($-1 - \alpha/2 \le x \le 0$) of the function is a parabola, which reaches its minimum at $x = -1\alpha/2$. Bellow this value of x the function is constant. The reasons for removing the part of parabola with negative slope from the model will be discussed in Section 3.1.

We start with the analysis of local bifurcations explaining the onset of stable subthreshold oscillations.

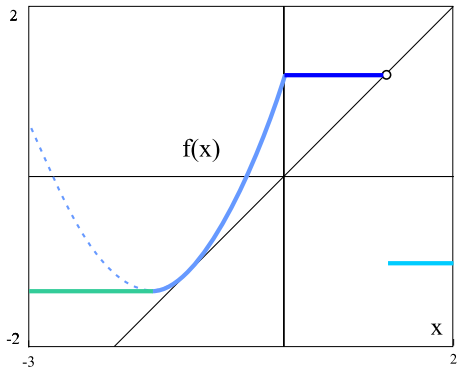

Figure 1: Function The initial parameter values are set so that the fast submap is next to the tangent bifurcation.

2.1 Birth of invariant curve

In the bifurcational analysis of fixed points we will restrict our consideration to the region $\alpha^2/2 - \alpha + y + \beta \leq x < 0$, i.e. to the parabolic segment of function (2). From (1a) one finds the x-coordinate of a fixed point which is given by $x_{fp} = \sigma - 1$. This "narrows" the parameter space to the region where $-\alpha/2 < \sigma < 1$. The y-coordinate of the fixed point in this region is given by $y_{fp} = (\sigma - 1)(1 - a) - \sigma^2 - \beta$.

Since this point is a single fixed one in the map, the further consideration is reduced to only two possible local bifurcations: a flip where one of multipliers equals -1, and the Andronov-Hopf bifurcation with a pair multipliers $e^{\pm i\varphi}$ on the unit circle, with $\varphi \neq \{0, \pi\}$.

The Jacobian matrix $\mathbf{J}$ evaluated at the fixed point is given by

$$\mathbf{J} = \begin{pmatrix} \alpha + 2\sigma & 1 \\ -\mu & 1 \end{pmatrix}.$$

The fixed point has the multipliers $\{\lambda_1 = -1, \lambda_2 = 1 - \mu/2\}$ on the flip-bifurcation curve whose equation is given $\alpha = -2\sigma - 1 - \frac{\mu}{2}$. It is worth noticing that the multipliers of the fixed point cross the imaginary axis when $\alpha = -2\sigma - \mu$.

In the case of the Andronov-Hopf (AH) bifurcation the Jacobian and the trace of $\mathbf{J}$ become 1 and $2\cos\varphi$, respectively. The equation of the corresponding bifurcation curve is given by

$$\alpha_{AH} = -2\sigma + 1 - \mu \tag{3}$$

On it the fixed point has a pair of complex conjugate multipliers:

$$\rho_{1,2} = 1 - \frac{\mu}{2} \pm \frac{i}{2}\sqrt{\mu(4-\mu)} = \cos\psi \pm i\sin\psi. \tag{4}$$

The fixed point is attracting at $\alpha < \alpha_{AH}$. Let us next determine the stability of the fixed point at the bifurcation. To do so we will need the first Lyapunov value L_1. If $L_1 < 0$ the point is stable, or unstable otherwise.

Introduce new coordinates in which the fixed point becomes the origin:

$$\begin{pmatrix} x \\ y \end{pmatrix} \mapsto \begin{pmatrix} x + 1 - \sigma \\ y + (\sigma - 1)(\alpha - 1) + \sigma^2 + \beta \end{pmatrix}.$$

The new map is now given by

$$\bar{x} = (1-\mu)x + x^2 + y, \qquad \bar{y} = y - \mu x. \tag{5}$$

Let us next make the transformation

$$\begin{pmatrix} x \\ y \end{pmatrix} \mapsto \begin{pmatrix} 0 & 1 \\ \sin\psi & 1 - \cos\psi \end{pmatrix} \begin{pmatrix} \xi \\ \eta \end{pmatrix},$$

with $\sin\psi$ and $\cos\psi$ defined in (4). This makes the linear part of (5) a rotation so that the map becomes the following form

$$\begin{pmatrix} \bar{\xi} \\ \bar{\eta} \end{pmatrix} = \begin{pmatrix} \cos\psi & -\sin\psi, \\ \sin\psi & \cos\psi, \end{pmatrix} \begin{pmatrix} \xi \\ \eta \end{pmatrix} + \begin{pmatrix} \frac{\cos\psi - 1}{\sin\psi} \\ 1 \end{pmatrix} \eta^2.$$

In variable $z = \xi + i\eta$ the map assumes the complex form

$$\bar{z} = ze^{i\psi} + \frac{c_{20}}{2}z^2 + c_{11}zz^* + \frac{c_{02}}{2}z^{*2} \tag{6}$$

with

$$c_{20} = \frac{1}{2}\left(\tan\frac{\psi}{2} - i\right), \quad c_{11} = \frac{1}{2}\left(i - \tan\frac{\psi}{2}\right), \quad c_{02} = \frac{1}{2}\left(\tan\frac{\psi}{2} - i\right). \tag{7}$$

The normalizing transformation

$$z \mapsto z - \frac{c_{20}}{e^{2i\psi} - e^{i\psi}}z^2 - \frac{c_{11}}{1 - e^{i\psi}}zz^* - \frac{c_{02}}{e^{-2i\psi} - e^{i\psi}}z^{*2}.$$

eliminates all the quadratic terms in (2.1). In the resulting normal form the coefficient L_1 at the desired cubic term

$$\bar{z} = e^{i\psi} z(1 + (L_1 + iS_1)zz^*) + O(\|z\|^3).$$

is the sought Lyapunov value. Its expression reads as follows:

$$L_1 = -\mathrm{Re}\frac{(1-2e^{i\psi})e^{-2i\psi}c_{20}c_{11}}{2(1-e^{i\psi})} - \frac{|c_{11}|^2}{2} - \frac{|c_{02}|^2}{4}. \tag{8}$$

Plugging (7) into (8) yields

$$L_1 = -\frac{1}{4}\frac{\cos(\psi)}{\cos(\psi)+1} = -\frac{2-\mu}{4(4-\mu)}$$

Thus, whenever the bifurcation curve AH is crossed transversally rightward the stable invariant curve emerges from the fixed point. Hence, we have a soft mechanism of generation of the subthreshold periodic oscillations, see Fig. 2.

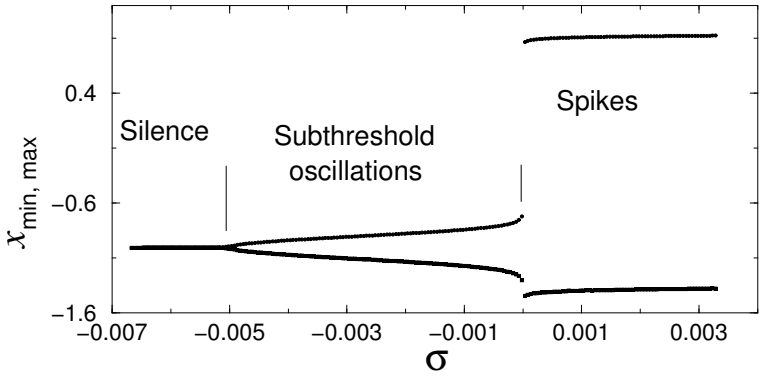

Figure 2: Bifurcation diagram illustrating the birth of "small" subthreshold oscillations and transition to spikes as parameter σ increases. The other parameters of the map are set as $a = 0.99$, $\beta = 0.0$ and $\mu = 0.02$.

2.2 Noise and subthreshold oscillations

To illustrate the dynamical features of the model let us now consider a typical neuronal behavior in the presence of of subthreshold oscillations mixed up

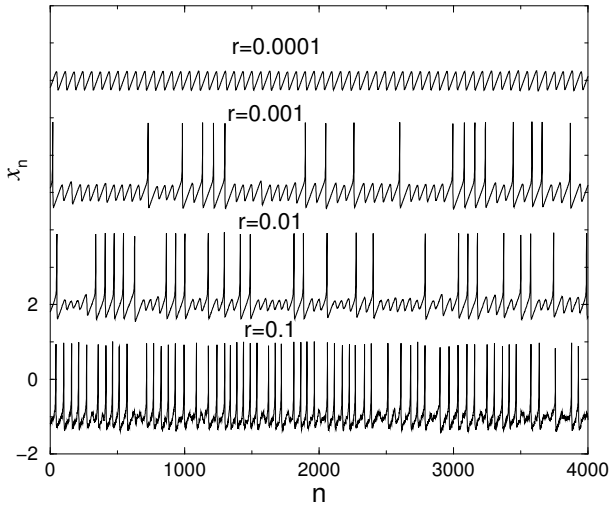

Figure 3: A variety of waveforms of iterates x_n in the map due to the influence by an external uniform random process of amplitude r injected into the fast map. Here $a = 0.99$, $\sigma = -0.0001$ and $\mu = 0.02$.

with an external noise. effects. It was observed recently that subthreshold periodic activity shapes stochastic properties of spiking in a neuron influenced by a noise, see [12, 13, 14, 15] for example.

Waveforms of map model (1) operating in the regime of subthreshold oscillations are shown in Fig. 3. The different traces correspond to different levels of noise r added into the first equation (1a). The top trace present the case where the level of noise is insufficient to induce the action potential (a spike). When the level of noise exceed a critical level the map starts producing occasional spikes. Such spikes are more likely to occur at the top of the oscillation. This results in the formation of multi-hump structure of the probability distribution function of interspike intervals (ISIs), see histograms shown in Fig. 4(a,b).

A further raise of the noise level increases the probability of action potentials. The spike fires almost every period of the subthreshold oscillation (see the bottom trace in Fig. 3). As the result, the probability density of ISIs has a single hump structure. These results are in a good agreement with the similar results obtained for ODE based models [14, 15].

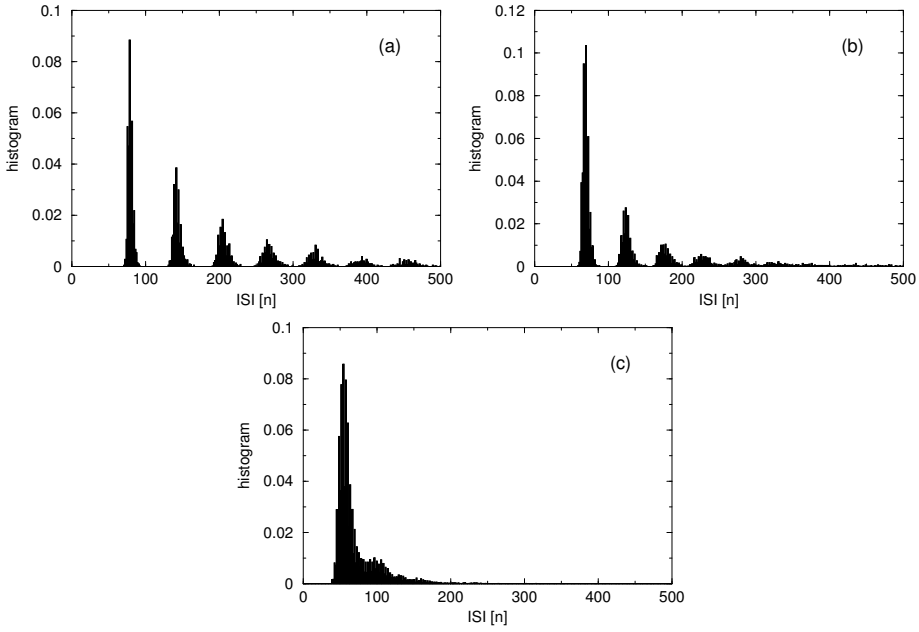

Figure 4: Histograms of interspike intervals (ISI) distribution computed for the waveforms shown in Fig. 2. (a) - $r = 0.001$; (b) - $r = 0.01$; (c) - $r = 0.1$.

3 Nontrivial effects of fast-slow dynamics in map model

Next we consider some interesting bifurcational aspects for a deeper understanding of map-based models with fast and slow dynamics.

3.1 Evolution of the invariant circle. "Period doubling"

Here we will examine the transition from these subthreshold oscillations (small stable invariant circle) to regular bursts (relatively large amplitude periodic orbits). It follows from the theory of canards that region of existence of the stable invariant circle is a narrow strip of width $\sim \mu$ adjoining the bifurcation curve AH. Furthermore, the nonstandard analysis clarifies that the size of the circle increases with the order 1 when a deviation from the Andronov-Hopf bifurcation is of order $e^{-1/\varepsilon}$. This means the stable in-

variant curve will grows abnormally fast, especially in the y-direction until it breaks down somehow.

To illustrate the saying and for sake of simplicity we replace the original map by a trivial normal form

$$\bar{x} = x + x^2 + y, \qquad \bar{y} = y - \mu(x - 1 + \sigma). \tag{9}$$

At $\mu = 0$ the fast subsystem is the simple parabolic map that possess all periodic doubling features. Variations in the parameter y shift the parabola vertically, see Fig. 5(b). This unimodal map has two fixed points that may disappear in the saddle-node bifurcation. Other then that the right point is remain always unstable. As y decreases the stable point loses the stability through the flip bifurcation yielding the initial push to the period doubling cascade. Let us try next to follows the evolution of the invariant curve in the singularly perturbed map. The smoothness of the invariant circle starts getting worse as its y-component becomes less or so then some y^* corresponding to the zero multiplier of the stable point in the fast map. The cycle breaks down finally as it enters the interval in y corresponding to the period doubling cascade in the fast system, see Fig. 5. This chaotic canard gets destroyed as a phase point crosses the unstable invariant set $\mathcal{S}^u$ which is an image of the unstable branch S_{pu} of fixed points of the unperturbed fast map. Supposing take a snapshot of the fast map could be taken in this moment, one would see how the bottom of the parabola is mapped right at the repelling fixed. If a bit higher, the unstable point is no longer the endpoint of the invariant interval, so the further iterations will escape from the attracting interval. As for the 2D map its successive self-adjustments fail to capture the trajectory, so it blows the chaotic attractor out, see Fig. 6.

We must say the existence of this chaotic set (chaotic canards) was not planed, neither was welcomed especially of the given size. Technically this moment is quite unlikely to be exposed unless one pays special efforts to do so such as evaluating the desired parameter value with prediction up to millionth fractions after the floating point. To avoid this fascinating but unwanted dynamics we introduced a lower threshold in the right-hand side of the function that should dump these chaotic oscillations.

3.2 Homoclinics Crossings

Now we return to the original map where two limiters are built in the function allowing no trajectory to run to infinity nor periodic doubling chaos.

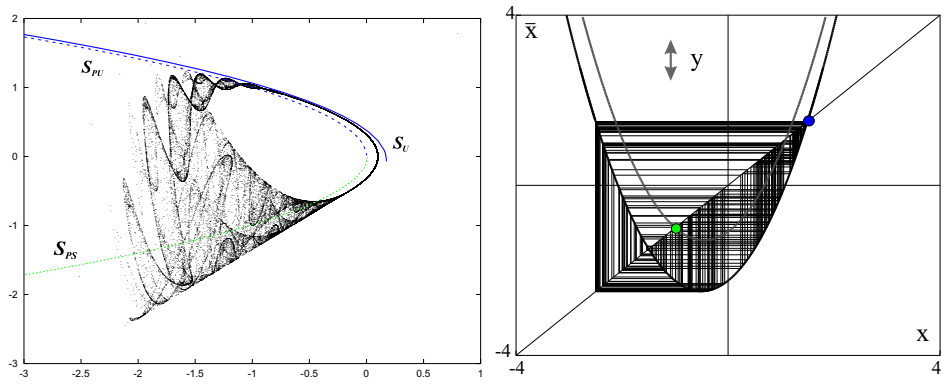

Figure 5: Chaotic set in the normal form 9 with $\sigma = s = 0.9499749\bar{9}$ and $\mu = 0.2$ explodes when it touches the unstable critical set $\mathcal{S}^u$. On the right – the corresponding momentary shot of the fast subsystem with $y = -2.2$. It captures the presence of homoclinics orbits to the repelling fixed point.

Here we discuss a way the subthreshold oscillations evolve into irregular spikes without noise. This delicate transition occurs within a sufficiently narrow parameter region that can be indeed widen by noise. The route is characterized by disappearance of the stable invariant circle replaced by co-existing low-amplitude subthreshold oscillations alternating with sporadic bursting protuberances. An example of chaotic dynamics is shown in Fig. 6.

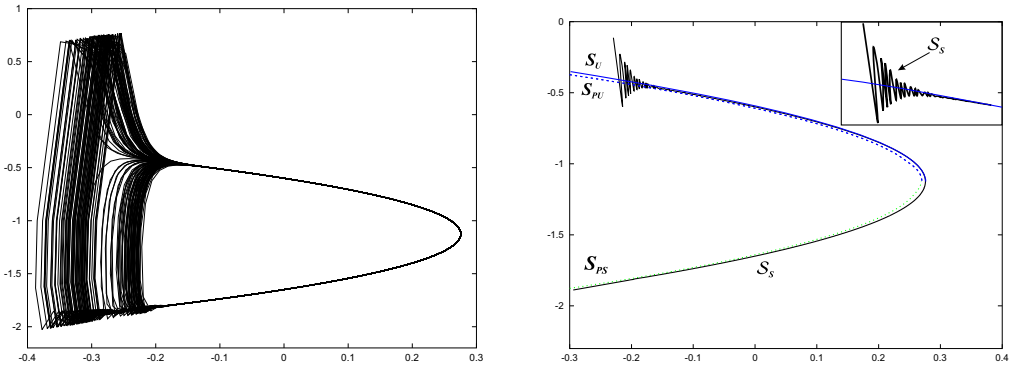

Figure 6: Chaos at $a = 1.25$, $\sigma = -0.13$ and $\mu = 0.02$ The wiggles of the stable critical set $\mathcal{S}_s$ increase as it follows the unstable critical set $\mathcal{S}_u$.

The transition mechanism is due to the heteroclinic crossings of the stable and unstable critical sets $\mathcal{S}^s$ and $\mathcal{S}^u$, like those sketched in Fig. 7. This

leads to formation of homoclinic wiggles and hence of a topological Smale horseshoe 7(b). Here homoclinic wiggles are caused by self-crossings, say, of $\mathcal{S}^s$ sketched in Fig. 7(b). This is one of many unusual features of two-dimensional endomorphisms. The reader may want to find more information in [16].

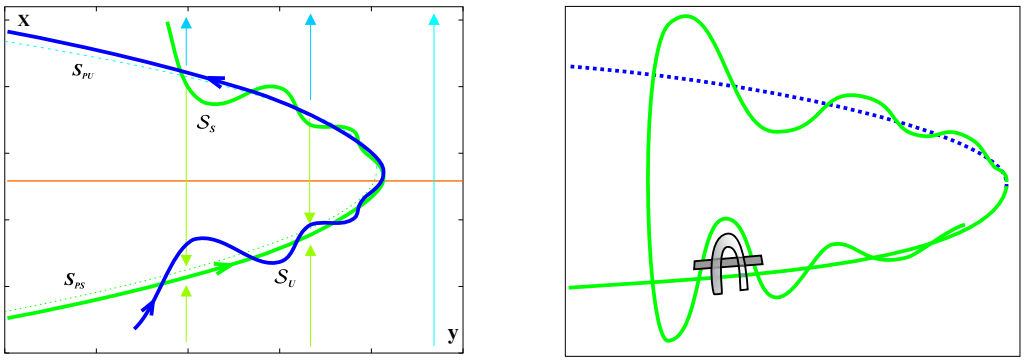

Figure 7: Homoclinic crossings of the critical sets $\mathcal{S}^s$ and $\mathcal{S}^u$. Self-crossings of the set $\mathcal{S}^s$, that are one of the features of noninvertible maps, may generate a topological Smale horseshoe.

4 Conclusion

It is shown that simple map-based model can be employed to replicate the behavior of neurons with subthreshold oscillations. This effect is achieved by special selection of nonlinear function in the fast subsystem. Dynamical mechanisms behind the transitions from silence to subthreshold oscillations of small amplitude and then to spiking activity are explained using the bifurcation approach.

Here we focused mostly of the individual dynamics of the map-based model. As the result we considered only the case when β and σ are some constants. One may notice from (1) that the parameter β can be eliminated by using the variable transformation $y + \beta \mapsto y$. However, the role of input parameter β is important only when time dependant input is considered instead, see [6] for detail. We would like to note that for studies of non-autonomous dynamics of this map model one needs to modify function (2) to insure that no trajectory of the system (1) gets locked in the interval

$0 < x < y + 1 + \beta$ as β or y increase. The discussion on suggested alterations of the function to resolve this obstacle can be found in [6].

5 Acknowledgment

N.R. was supported in part by U.S. Department of Energy (grant DE-FG03-95ER14516). A.S. acknowledges the RFBR grants No. 02-01-00273 and No. 01-01-00975.

References

[1] D.R. Chialvo, *Chaos, Solitons and Fractals* **5**, 461 (1995).

[2] B. Cazelles, M. Courbage, and M. Rabinovich, *Europhys. Lett.* **56**, 504 (2001).

[3] N.F. Rulkov, *Phys. Rev. Lett.* **86**, 183 (2001)

[4] K.V. Andreev and L.V. Krasichkov *Izv. Akad. Nauk Fiz.* **66**, 1777 (2002).

[5] E.M. Izhikevich and F.C. Hoppensteadt, Bursting Mappings, submitted for publication. 2003

[6] N.F. Rulkov, *Phys. Rev. E* **65**, 041922 (2002).

[7] N. F. Rulkov, M.V. Bazhenov, and A. L. Shilnikov, Proceedings of International Symposium on Topical Problems of Nonlinear Wave Physics, Russia, September 2003.

[8] A. L. Shilnikov and N.F. Rulkov, *Int. J. Bif. Chaos* **13**, 11 (2003).

[9] R. Llinás, *Science* **242**, 1654 (1988).

[10] R. Llinás and Y. Yarom, *Journal of Physiology* **315**, 549 (1981).

[11] R. Llinás and Y. Yarom, *Journal of Physiology* **376**, 163 (1986).

[12] V.A. Makarov, V.I. Nekorkin, and M.G. Velarde, *Phys. Rev. Lett.* **86**, 3431 (2001).

[13] M.G. Velarde, V.I. Nekorkin, V.B. Kazantsev, V.I. Makarenko, and R. Llinás, *Neural Networks* **15** 5 (2002).

[14] D.T.W. Chik, Y. Wang and Z.D. Wang, *Phys. Rev.* E, **64**, 021913 (2001).

[15] E.I. Volkov, E. Ullner, A.A. Zaikin, and J. Kurths, *Phys. Rev.* E, **68**, 026214 (2003).

[16] Mira, C. Gardini, L., Barugola, A. and Cathala, J.-C. [1996] *Chaotic dynamics in two-dimenional noninvertable maps,* World Scientific (Singapore, New Jersey, London).

6 Appendix: Inverse map

To locate the unstable set $\mathcal{S}^u$ which is a surface of slow motion one should consider the inverse map $F_{inv} : (x, y) \mapsto (\bar{x}, \bar{y}) \in D$ defined in $D := \{-1 - \alpha/2 \leq x \leq 0\}$. Within D the inverse F_{inv} assumes the following form

$$\bar{x} = \alpha x + (x+1)^2 + y + \beta, \tag{10a}$$

$$\bar{y} = y - \mu(x + 1 - \sigma). \tag{10b}$$

Subtracting (10b) from (10a) one gets

$$\bar{x} - \bar{y} = \alpha x + (x+1)^2 + \mu(x + 1 - \sigma) + \beta. \tag{11}$$

Solving it for x one can find x as a the following function in $\bar{x}$ and $\bar{y}$

$$x = -(2 + \alpha + \mu)/2 + \sqrt{(2 + \alpha + \mu)^2/4 - (1 + \beta + \mu(1 - \sigma) - \bar{x} + \bar{y}}. \tag{12}$$

To get the equation for the y-variable expression (12) must be plugged into (10b).